Polynomial Control Strategy of the DC/DC converter for Energy share between Supercapacitors and Battery

M.B.Camara, B.Dakyo, *Member IEEE*, C. Nichita

***Abstract* -- This paper deals the embedded energy share between Supercapacitors (SC) and batteries. SC modules are dimensioned for peak power requirement and batteries provide the power in steady state. This last is directly connected to the DC-bus to maintain the voltage level between 38V and 60V. A buck-boost converter is interfaced between the SC and the DC-bus to manage the available energy. The originality of this study is focused on energy management strategy between SC and batteries. The proposed strategy is based on polynomial (RST) controller. Due to cost and available components (no optimized) such as batteries and semiconductors, the experimental test bench is designed in reduced scale. The used packs of SC include two modules of 10 cells in series for each one, and present a maximum voltage of 27V. The buck-boost converters control algorithms are implemented in PIC18F4431 microcontroller. Experimental and simulation results obtained from polynomial control strategy are presented, analyzed, and compared to proportional integral ones.**

***Index Terms*-- Batteries; Buck-boost converter; Dynamic control; Energy management; Energy storage; Electric Hybrid vehicle (HEV); Polynomial control strategy; Supercapacitors.**

I. NOMENCLATURE

V_{bat}	Battery's voltage
V_{bus1}	DC-bus voltage
V_{sc1}, V_{sc2}	Supercapacitors modules voltages
I_{bat}	Battery's current
I_{batref}	Battery's current reference
I_{ch}	Electric load current
I_L	DC-bus current from Supercapacitors
I_{bus1}	Contribution of the first SC module to DC-bus current
I_{bus2}	Contribution of the second SC module to DC-bus current
I_{sc1}, I_{sc2}	First and second *S*C modules currents
I_{sc1ref}, I_{sc2ref}	Supercapacitors currents references
α_1	Boost converter mode duty cycle
α_2	Buck converter mode duty cycle
L_1, L_2	SC currents smoothing inductors (50µH)
C_1, C_2	DC-bus voltage smoothing capacitor (1500 µF)
λ	Battery's current smoothing inductor (25µH)
f	Converter Control frequency (10kHz)
η_1, η_2	Two parallel boost converters efficiencies
$\eta_{p\text{-}RST}$	Boost converters global efficiency
ω_n	Dynamic control band-width in [rad/s]
T_e	Sampling period in [s]
HEV	Electric Hybrid Vehicle
RST	Controller name from $R(z^{-1})$, $S(z^{-1})$ and $T(z^{-1})$

M. B. Camara, B. Dakyo and C. Nichita are with the GREAH (Groupe de Recherche en Electrotechnique et Automatique du Havre) Laboratory, University of Le Havre, 76600 Le Havre, FRANCE, Phone: 33 (0)2 32 74 43 25; Fax: 33 (0)2 32 74 43 48, http://www.univ-lehavre.fr, (e-mail: camaram@univ-lehavre.fr, brayima.dakyo@univ-lehavre.fr)

II. INTRODUCTION

THESE last 10 years, many researches are undertaken for HEV autonomy and performances improvement. The battery and supercapacitors (SC) mixture Figure.1, with a good energy management between these devices enables to reduce the battery size and improves its lifetime [1]. This solution is very promising in the short and medium term, due to SC high dynamic performances and their lifetime about 10 years, higher compared to battery ones. Also, these high power storage devices present less risk of pollution than the battery.

The main contribution of this paper is focused on a novel strategy of embedded energy management, using polynomial (RST) controllers. This last gives a robust algorithm, with good performances in the following case of process: with a pure delay, whose dynamic characteristics change during operation, and where the reference should not be exceeded.

To validate the proposed method, two SC modules and buck-boost converters are designed in the reduced scale. This solution is due to reason of cost and available components such as, the batteries and the semiconductors. The designed converters are controlled by PIC18F4431 microcontroller with a compiler of type *PCW-C-Compiler-IDE*. The experimental data acquisition system is monitored by using National Instruments Labview software and *PXI-1002* unit.

III. DC/DC CONVERTERS MODELING AND CONTROL

The main goal of this paragraph consists to establish the DC/DC converters control laws for energy share between the SC and battery. This study is focused on two buck-boost [1]-[6] converters with parallel topology. The SC modules are connected to DC-link, via these bidirectional converters, which ensure the SC charge and discharge. The proposed dynamic control strategy is based on the converter's duty cycles estimation. The used converter topology [2], [3], [4] is presented in Figure.2.

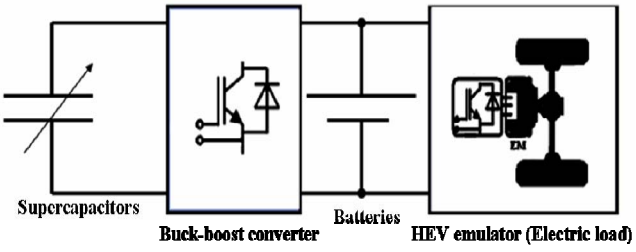

Figure.1: Supercapacitors and Battery HEV topology

978-1-4244-4175-4/10/$25.00 ©2010 IEEE

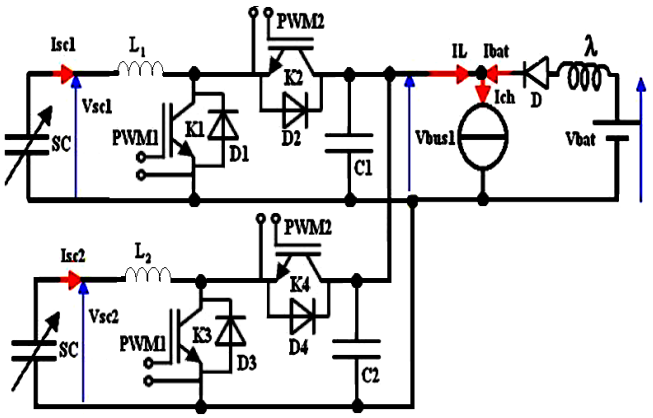

Figure.2: Buck-boost converters configuration

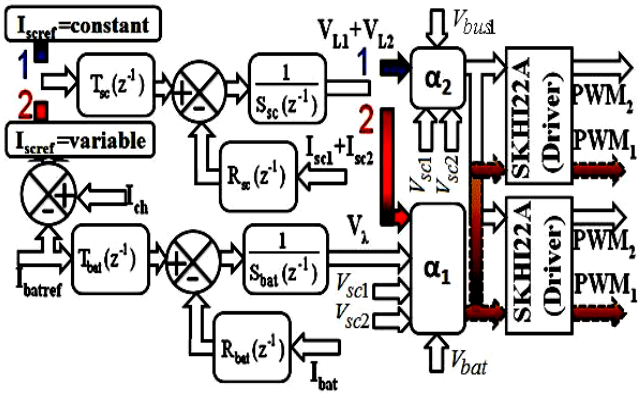

Figure.3: Implemented polynomial control for buck and boost converters

A. *Converter modeling*

To establish the bidirectional converter model, the buck and boost [5], [6] converters operating modes must be analyzed. During buck converter mode, K2 and K4 semiconductors are ON, while K1 and K3 are OFF. Contrary to this mode, K1 and K3 are ON, while K2 and K4 became OFF.

For this study, the following currents: I_{sc1}, I_{sc2}, I_L, I_{bus1} and I_{bus2} are assumed negative during the SC energy storage (buck converter mode), and they are positive during the SC discharge (boost converter mode). The buck-boost converter average model resulting from the buck/boost converter analysis is given in (1). In this analytical model, k and α variables can have the following values:

$$\begin{cases} V_{L1} = L_1 \cdot \frac{d}{dt}(I_{sc1}) = k \cdot (V_{sc1} - \alpha \cdot V_{bus1}) \\ V_{L2} = L_2 \cdot \frac{d}{dt}(I_{sc2}) = k \cdot (V_{sc2} - \alpha \cdot V_{bus1}) \\ V_{\lambda} = \lambda \cdot \frac{d}{dt}(I_{bat}) = V_{bat} - V_{bus1} \end{cases}, \begin{cases} I_L = I_{bus1} + I_{bus2} \\ I_{ch} = I_{bat} + k \cdot I_L \\ I_{sc} = I_{sc1} + I_{sc2} \end{cases} \quad (1)$$

- Boost converter mode: $k = 1$ and $\alpha = 1 - \alpha_1$, where α_1 is the boost converter duty cycle average value.
- Buck converter mode: $k = -1$ and $\alpha = \alpha_2$, where α_2 is the buck converter duty cycle average value.

This average model is nonlinear because of crosses between the control variables (α_1, α_2) and the state variables (I_{sc1}, I_{sc2} and V_{bus1}) as presented in Figure.3. The V_{sc1}, V_{sc2}, V_{bus1}, I_{ch} and V_{bat} variables are likely to disturb the control; they must be measured and used in the control laws estimation to ensure a dynamic control. This nonlinear behavior is studied in [4]. The bidirectional converter control laws resulting from the boost and buck converters modeling are respectively defined by α_1 and α_2 as presented in (2).

$$\begin{cases} \alpha_1 = 1 - \frac{1}{2} \cdot \frac{(V_{sc1} + V_{sc2}) - (V_{L1} + V_{L2})}{(V_{bat} - V_{\lambda})} \\ \alpha_2 = \frac{1}{2} \cdot \frac{(V_{L1} + V_{L2}) + (V_{sc1} + V_{sc2})}{V_{bus1}} \end{cases} \quad (2)$$

B. *Polynomial (RST) Control Strategy*

This study is based on the polynomial (RST) dynamic control strategy [7]-[9] of the buck-boost converters, for energy share between battery and SC. The proposed control strategy is the current type because the DC-link voltage level is fixed by battery. The control strategy illustrated in Figure.3 presents two distinct modes:

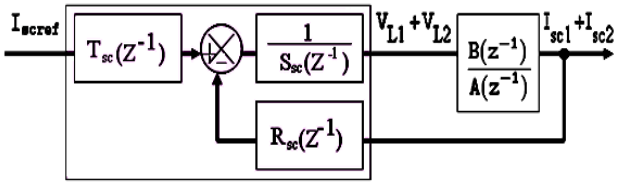

Figure.4: r_{0sc} and r_{1sc} estimation for two converters control

The first is characterized by the charge of the SC with constant current ($I_{scref} = constant$). During this operation, the battery current loop is not activated, i.e. only the PWM2 signal is activated (**1** is ON, and **2** is OFF). In this state, one only polynomial controller is used.

The second operation is characterized by the discharge of the SC with variable current. The SC reference current presented in (3) is obtained from energy management between battery and SC, where η_1 and η_2 present the two parallel boost converters theoretical efficiencies (100% for simulations). During this operation the battery and SC current loops with PWM1 control signal are activated (**1** is OFF, and **2** is ON). In this case, two controllers are used for SC and battery currents control. During this operation, PWM1 and PWM2 signals cannot be activated simultaneously.

$$\begin{cases} I_{sc1ref} = \frac{1}{2} \cdot \frac{V_{bus1}}{\eta_1 \cdot V_{sc1}} \cdot (I_{ch} - I_{batref}) \\ I_{sc2ref} = \frac{1}{2} \cdot \frac{V_{bus1}}{\eta_2 \cdot V_{sc2}} \cdot (I_{ch} - I_{batref}) \\ I_{scref} = I_{sc1ref} + I_{sc2ref} \end{cases} \quad (3)$$

For polynomial parameters estimation, the sampling process transfer functions obtained from (1) is presented in (4).

$$\begin{cases} G_1(z^{-1}) = \frac{I_{sc1}(z^{-1})}{V_{L1}(z^{-1})} = \frac{T_e}{L_1} \cdot \frac{z^{-1}}{1 - z^{-1}} \\ F(z^{-1}) = \frac{I_{bat}(z^{-1})}{V_{\lambda}(z^{-1})} = \frac{T_e}{\lambda} \cdot \frac{z^{-1}}{1 - z^{-1}} \\ G_2(z^{-1}) = \frac{I_{sc2}(z^{-1})}{V_{L2}(z^{-1})} = \frac{T_e}{L_2} \cdot \frac{z^{-1}}{1 - z^{-1}} \end{cases}, \quad (4)$$

The converters control strategy can be simplified if $L_1 = L_2$ and general transfer function resulting from this assumption is presented in (5).

$$G_1(z^{-1}) = G_2(z^{-1}) = \frac{I_{sc1}(z^{-1}) + I_{sc2}(z^{-1})}{V_{L1}(z^{-1}) + V_{L2}(z^{-1})} \quad (5)$$

Polynomial control method, consists in identifying $R(z^{-1})$,

$S(z^{-1})$ and $T(z^{-1})$ polynomials from an imposed model in closed loop, where $R(z^{-1})$ and $S(z^{-1})$ ensure the role of the regulation and $T(z^{-1})$ ensures the system control. The $R(z^{-1})$ and $S(z^{-1})$ polynomials are identified from Diophantine equation [7]. $G_1(z^{-1})$ and $F(z^{-1})$ transfers functions in closed loop are similar this is why one only method is presented for $R(z^{-1})$, $S(z^{-1})$ and $T(z^{-1})$, polynomials identification by using $G_1(z^{-1})$. The desired polynomial in closed loop is given in (6).

$$P(z^{-1}) = \left(1 - z^{-1} \cdot \exp\left(-\omega_n \cdot T_e\right)\right)^2 \tag{6}$$

This function is of second order, and then the closed loop transfer function characteristic equation must be equal to second order. In other words, the order of $A(z^{-1})$ and $B(z^{-1})$, is equal to 1, and that of $R(z^{-1})$ and $S(z^{-1})$, must also be equal to 1. The SC current control polynomial must be obtained by using closed loop system presented in Figure.4. In this case, the balancing issue between I_{sc1} and I_{sc2} is no significant when the two SC modules are balanced, and when the two converters are same. From $G_1(z^{-1})$, it is possible to write the numerator and denominator as presented in (7).

$$\begin{cases} A(z^{-1}) = 1 - z^{-1} \\ B(z^{-1}) = \dfrac{T_e}{L_1} \cdot z^{-1} \end{cases} \tag{7}$$

To obtain a minimal static error in HEV energy share with a disturbance rejection, $R(z^{-1})$ and $S(z^{-1})$ polynomials presented in (8) are selected.

$$\begin{cases} S(z^{-1}) = 1 - z^{-1} \\ R(z^{-1}) = r_{0sc} + r_{1sc} \cdot z^{-1} \end{cases} \tag{8}$$

The sampling process transfer function resulting from system closed loop is given in (9).

$$F_{cl}(z^{-1}) = \frac{T(z^{-1}) \cdot B(z^{-1})}{A(z^{-1}) \cdot S(z^{-1}) + B(z^{-1}) \cdot R(z^{-1})} \tag{9}$$

In goal to simplifying the control algorithm and reduce the number of parameters which must be identified [8], [9], $T(z^{-1})$ is assumed equal to $R(z^{-1})$. The coefficients of this polynomial are identified, using a comparison between $P(z^{-1})$ and the denominator of the transfer function in closed loop as expressed in (10).

$$P(z^{-1}) = A(z^{-1}) \cdot S(z^{-1}) + B(z^{-1}) \cdot R(z^{-1}) \tag{10}$$

To ensure a robust stability of the system, the closed loop poles must be remaining inside the unit circle (discrete time case) for all the models (Figure.5.a). About the robust performance evaluation, the closed loop poles must be remaining inside the circle (c,r) as presented in Figure.5.b. The obtained poles from this method, using (6) are plotted in Figure.5.c. This curve shows that the conditions of stability and robust performance are respected.

Equation (11) presents the SC currents loop polynomials approximate coefficients, according to L_1 inductor, T_e sampling period, and the band-width ($\omega_n \geq Log(2)/Te$).

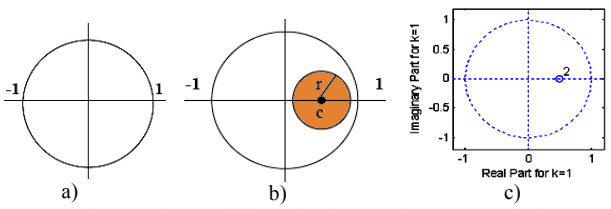

Fig.5: Robust stability and robust performance analysis

To choose r_{0sc} and r_{1sc} coefficients, inside the bandwidth, a k parameter is introduced as presented in following equation $\omega_n = k.Log(2)/Te$. This variable is selected between 1 and 2, and it gives all possible values of the bandwidth.

$$\begin{cases} r_{0sc} = 2 \cdot \left(1 - \exp\left(-\omega_n \cdot T_e\right)\right) \cdot \dfrac{L_1}{T_e} \approx 2 \cdot \left(1 - \dfrac{1}{1 + \omega_n \cdot T_e}\right) \cdot \dfrac{L_1}{T_e} \\ r_{1sc} = \left(\exp\left(-2 \cdot \omega_n \cdot T_e\right) - 1\right) \cdot \dfrac{L_1}{T_e} \approx \left(\dfrac{1}{1 + 2 \cdot \omega_n \cdot T_e} - 1\right) \cdot \dfrac{L_1}{T_e} \end{cases} \tag{11}$$

$G_1(z^{-1})$ and $F(z^{-1})$ discretized processes are similar, in other word the battery current loop polynomials coefficients can be obtained while replacing L_1 by λ in (11). This operation enables to write the battery current control polynomial approximate coefficients (12).

$$\begin{cases} r_{0bat} \approx 2 \cdot \left(1 - \dfrac{1}{1 + \omega_n \cdot T_e}\right) \cdot \dfrac{\lambda}{T_e} \\ r_{1bat} \approx \left(\dfrac{1}{1 + 2 \cdot \omega_n \cdot T_e} - 1\right) \cdot \dfrac{\lambda}{T_e} \end{cases} \tag{12}$$

These coefficients are respectively implemented in Hybrid system model for simulations, and in PIC18F4431 microcontroller for experimental validation.

C. *Simulation Results*

The used models of the SC and battery are presented in previous papers [1], [4]. Due to performances of the used computer, only the traction mode is simulated. In this condition, the reference of the battery current I_{batref} is fixed at 5A so that, the SC modules provide HEV energy request during the transient states.

The load current (Figure.6.a) sharing between the battery and SC is plotted in Figure.6.b. The DC-link current I_L is ensured by two SC modules. The first boost converter (K1-D2) ensures 50% and the second (K3-D4) ensures also 50% of I_L. This figure shows that the battery current control strategy is satisfactory during 40 seconds, after that it becomes insufficient because the SC discharges.

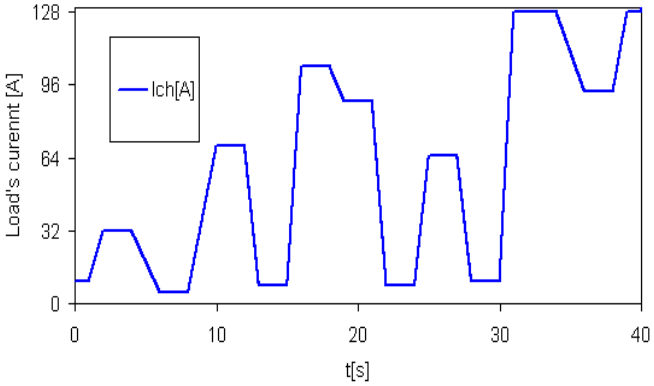

Figure.6. a: Load current (I_{ch}) profile

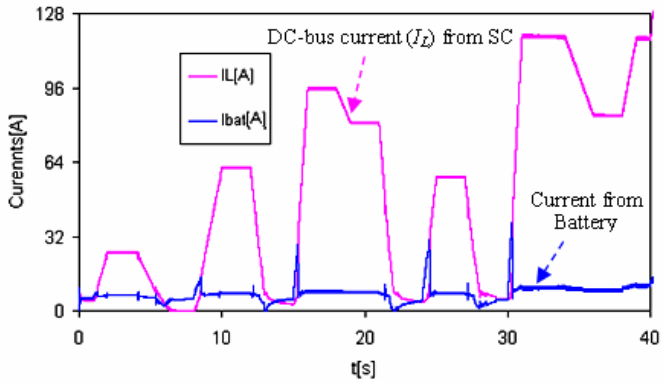

Figure.6.b: Battery current (I_{bat}) and DC-bus current (I_L) from SC

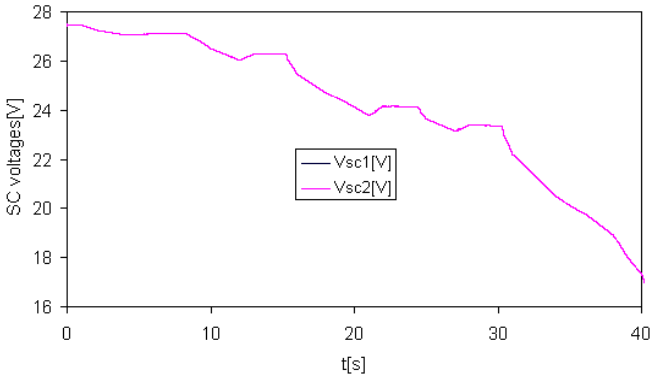

Fig.7: SC modules voltages with $V_{sc1} = V_{sc2}$

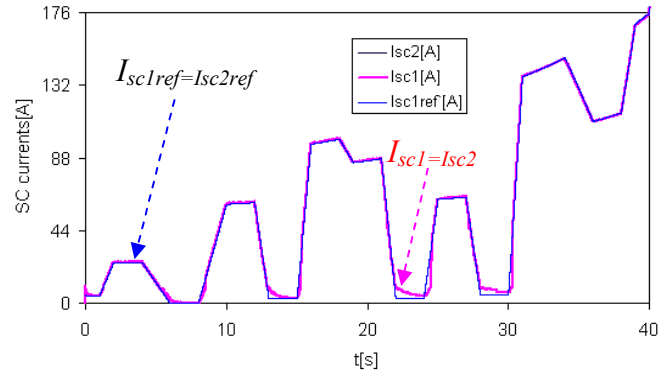

Figure.8: Supplied current of two SC modules where $I_{sc1} = I_{sc2}$, and $I_{sc1ref} = I_{sc2ref}$.

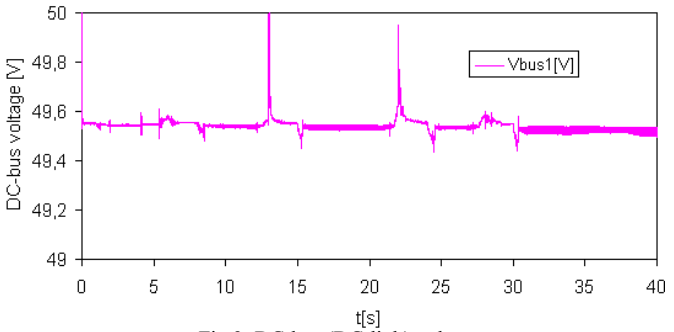

Fig.9: DC-bus (DC-link) voltage

Figure.7 presents the SC modules voltages simulation results during HEV traction states. These voltages are same and they show that the used model for HEV behavior simulation is satisfactory. Figure.8 presents the simulation results of the two modules currents, where I_{sc1} and I_{sc2} are identical. These curves show that the control strategy of the SC currents (I_{sc1} and I_{sc2}) is satisfactory during HEV traction state, and these currents are very close to their references (I_{sc1ref} *and* I_{sc2ref}). DC-link voltage V_{bus1} simulation result is plotted in Figure.9. This curve shows the efficiency of the battery coupled on the DC-bus to maintain the voltage level between the 38V-60V.

IV. DC/DC Converters Design and Experimentation

A. Experimental setup

The experimental test bench designed for theoretical study validation is presented in Fig. 10. This test bench includes two SC modules, a battery module, and buck-boost converter, which ensure energy share between battery and SC. The minimum and maximum voltages of the SC modules are respectively limited to 18V and 27V. The battery module, which maintains the DC-link voltage level, has a rated voltage of 48V (i.e., fours batteries of 12V in series). This level is assumed allowed when it is included between 38V and 60V. An electronics load is used to simulate the HEV energy request in traction mode. The used components with the voltage levels of supercapacitors and the battery are summarized in TABLE I.

The proposed control strategy consists to store all measurement errors samples of the current from supercapacitors, to estimate the voltage drop in the L_1 and L_2 inductors as presented in Figure.3. To do these estimations, it is necessary to provide to algorithm the global reference of the supercapacitors current I_{scref}, the polynomial coefficients (r_{0sc}, r_{1sc}) and initial voltage of the $V_{L1}(n)+V_{L2}(n)$. The implemented algorithm for supercapacitors current control is expressed in (13), where n is the samples numbers.

$$\begin{cases} \Delta I_{sc}(n) = I_{scref}(n) - I_{sc}(n) \\ V_{L1}(n+1) + V_{L2}(n+1) = V_{L12}(n+1) \\ V_{L1}(n) + V_{L2}(n) = V_{L12}(n) \\ V_{L12}(n+1) = V_{L12}(n) + r_{0sc} \cdot \Delta I_{sc}(n+1) + r_{1sc} \cdot \Delta I_{sc}(n) \\ \Delta I_{sc}(n+1) = I_{scref}(n+1) - I_{sc}(n+1) \end{cases} \quad (13)$$

The control algorithm of the current from the batteries is similar to supercapacitors ones as showed in (14). To estimate V_λ(n + 1), it is necessary to provide to system, the battery's current reference I_{batref}, the polynomial coefficients (r_{0bat} , r_{1bat}), and initial voltage of the V_λ(n).

$$\begin{cases} \Delta I_{bat}(n) = I_{batref}(n) - I_{bat}(n) \\ V_\lambda(n+1) = V_\lambda(n) + r_{0bat} \cdot \Delta I_{bat}(n+1) + r_{1bat} \cdot \Delta I_{bat}(n) \\ \Delta I_{bat}(n+1) = I_{batref}(n+1) - I_{bat}(n+1) \end{cases} \quad (14)$$

These algorithms are implemented in PIC18F4431 microcontroller, with a frequency of 10 kHz, for buck-boost converter control.

TABLE I
TEST BENCHES COMPONENTS NOMENCLATURE

Symbol	Name	Value
L_1=L_2=L	SC currents smoothing inductors	50 µH
C_1=C_2=C	DC-bus voltage filtering capacitors	1500 µF
λ	Battery current smoothing inductor	25 µH
V_{sc1}, V_{sc2}	SC modules voltages	18-27 V
Vbus1	DC-bus voltage	38-54
SC_1=SC_2	Symbol of the SC modules	-

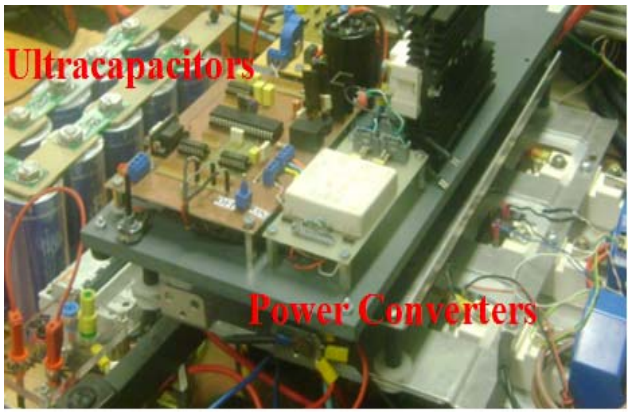

Fig. 10: Experimental setup for SC-lithium battery energy management

TABLE II
SUPERCAPACITORS AND BATTERY CURRENTS CONTROLLERS PARAMETERS

Symbol	Value	Name
Te=1/f	100µs	Sampling period
$r_{0sc} + r_{1sc}.z^{-1}$	$0.3858 - 0.2784.z^{-1}$	(I_{sc1}) and (I_{sc2}) control polynomial
$r_{0bat} + r_{1bat}.z^{-1}$	$0.1929 - 0.1392.z^{-1}$	(I_{bat}) control polynomial
$P(z^{-1})$	$1-1.2284.z^{-1}+ 0.4432 .z^{-2}$	Desired polynomial

The used parameters are presented in TABLE II, and the tests are carried out for two charge cycles with a constant current (I_{scref}=60A, i.e., I_{sc1ref}=30A and I_{sc2ref}=30A) and two cycles of discharge with a variable current for each module.

B. *Experimental test conditions and results*

Conventionally, I_{sc1}, I_{sc2}, I_L, I_{bus1}, and I_{bus2} currents are considered negative during the SC charging, and they are positive during the discharge operation. To show the bidirectional behavior of the converters, the SC modules are charged and discharged with constant current and variable current respectively. The charging mode corresponds to SC energy storage, and that of the discharge corresponds to SC energy supply to DC-bus. If the modules are discharged more than 75%, the dynamic control becomes insufficient because of the low level of the SC voltage.

For all experimental tests, the minimum and maximum voltages of the modules are respectively fixed at 18V and 27V. The HEV current request I_{ch} is fixed at 50A. The reference currents during the modules charge and discharge are respectively I_{scref}=60A (30A for each module) in buck mode, and I_{batref} = 10A in boost mode.

The SC voltages V_{sc1} and V_{sc2} values are identical as plotted in Figure.11.a. The I_{sc1} and I_{sc2} currents are also identical except during the discharge when a light difference appears because of the imbalanced impedances of the two parallel boost converters. This difference is due to no optimized wiring. The converter, which disposes lowest impedance, provides the largest current as presented in Figure.11.b.

During the SC discharge (Figure.12), i.e. between 80 seconds and 135 seconds, the battery current reference I_{batref} is fixed at 10A so that, the SC modules provide HEV energy request (I_{ch}) during the transient states via buck-boost converters. The dynamic control results of the DC-link current I_L from SC, and voltage obtained from these experimental tests conditions are showed in Figure.13. In this case, each converter ensures 20A, and the remainder current (10A) is provided by the battery as presented in Figure.12.

The two parallel boost converters experimental efficiency, obtained from (15) is presented in Figure.14.

$$n_{p\_RST} = \frac{(I_{bus1} + I_{bus2}) \cdot V_{bus1}}{I_{sc1} \cdot V_{sc1} + I_{sc2} \cdot V_{sc2}} \quad (15)$$

This figure shows, when $I_{sc1}+I_{sc2}$=80A, the boost converters efficiency is 86% approximately. However, it is possible to improve this value by optimizing the wiring and using low losses power semiconductors.

These experimental results at a reduced scale show that the proposed energy management strategy is satisfactory, and this strategy can be extrapolated to Hybrid Electric Vehicle embedded energy share.

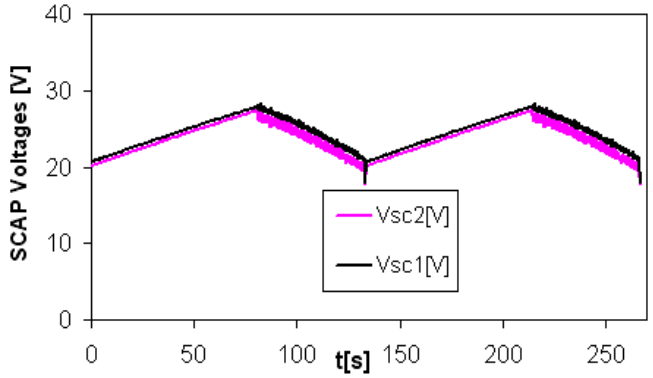

Figure.11.a: SC modules Voltages with $V_{sc1} \approx V_{sc2}$

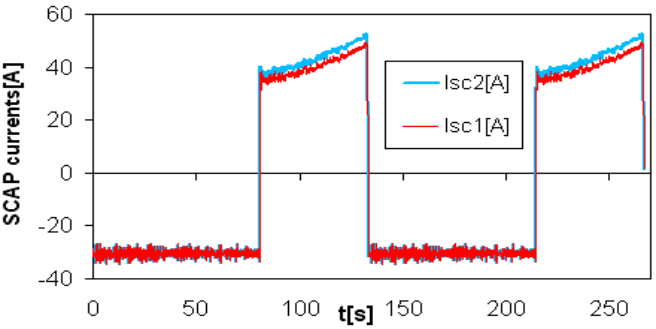

Figure.11.b: SC modules currents with $I_{sc1} \approx I_{sc2}$

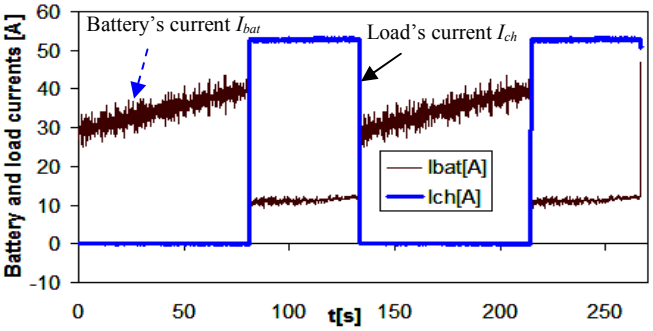

Figure.12: Battery and electronics load currents

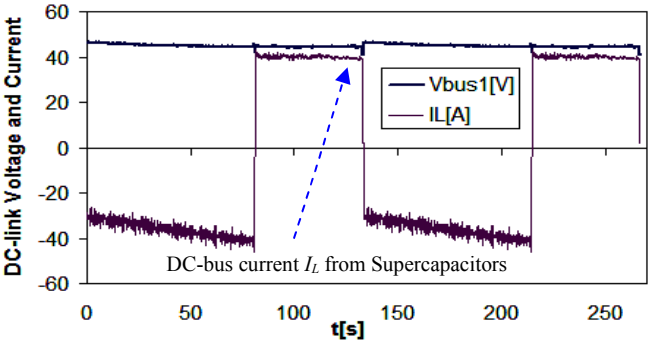

Figure.13: DC-bus voltage and current from SC

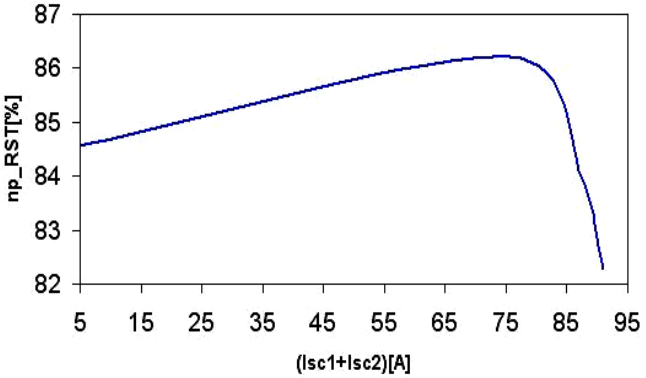

Figure.14: Two parallel boost converters efficiency

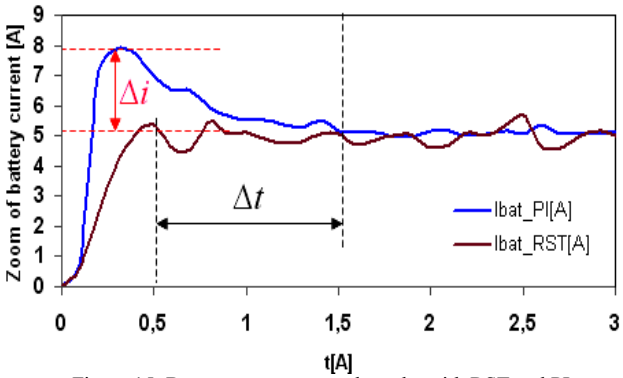

Figure.15: Battery current control results with RST and PI

C. *Advantages of the polynomial controller compared to Proportional Integral (PI)*

To illustrate the advantages of polynomial controller, compared to classical PI, the experimental tests are carried out using boost converter configuration Figure.2, where PWM2 is OFF. To do this comparison, the polynomial and PI controllers are implemented in PIC18F4431 microcontroller to control the boost converters. These controllers are estimated in identical conditions.

In the case of these tests, the battery current reference is $I_{batref}=5A$, so that the SC provide to HEV the significant power during transient states. To simulate the HEV behavior a power electronic load (I_{ch}) is used with a current of 25A.

Figure.15 shows, the battery current resulting from polynomial control is more interesting than that of classical PI, i.e., the PI control result presents a delay $\Delta t=1s$ compared to polynomial system. About initial conditions, the polynomial control strategy is also interesting compared to PI as presented in Figure.15, where $\Delta i=3A$, either 60% of I_{batref}. These curves show, the polynomial control is more accurate and robust than classical PI.

These experimental results enable to conclude, the proposed control strategy is more performing (rapid and accurate) compared to PI applied in hybrid vehicle applications.

V. Conclusion

An original strategy of the RST synthesis with polynomial's coefficients estimation according to inductors, sampling period, and desired bandwidth, is presented in this paper. This polynomial control strategy is applied to buck-boost converters, for energy share between SC and battery.

The resulting algorithms are robust and easy to do with a microcontroller or DSP devices. In the case of this study, the proposed algorithms are implemented in PIC18F4431 microcontroller for bidirectional converters control. The advantages of the polynomial control strategy compared to classical PI techniques applied in HEV applications are highlighted.

The simulation and experimental results at a reduced scale show that, the proposed energy management strategy is satisfactory, and this strategy can be extrapolated to Hybrid Electric Vehicle embedded energy management.

VI. References

[1] M.B. Camara , H. Gualous, F. Gustin, A. Berthon, B.Dakyo, "DC/DC converters design for Supercapacitors and Battery Power management in Hybrid Vehicle Applications-Polynomial Control Strategy", *IEEE Trans. On Industrial Electronics*, Vol.57, No.2, February 2010

[2] M.B. Camara, H. Gualous, F. Gustin, and A. Berthon. "Control strategy of hybrid sources for transport applications using supercapacitors and battery". *IEEE, IPEMC2006*, 13-16 August, Shanghai, P.R.CHINA, Volume 1, pp.1–5, 2006.

[3] L. Solero, A.Lidozzi, J.A.Pomilo, "Design of Multiple-Input Power Converter for Hybrid Vehicles", *IEEE Trans. on Power Electronics*, Vol.20, N.5, September 2005

[4] Camara, M.B., Gualous, H., Gustin, F. and Berthon, A. "Design and New Control of DC/DC Converters to share energy between Supercapacitors and Battery in Hybrid Vehicle", *IEEE Trans. on Vehicular Technology,* vol.57, no 5, pp.2721-2735, September 2008.

[5] Song-Yul Choe, Jong-Woo Ahn, Jung-Gi Lee, and Soo-Hyun Baek "Dynamic Simulator for a PEM Fuel Cell System With a PWM DC/DC Converter", *IEEE Trans. on Energy Conversion,* vol.23, no 2,June 2008.

[6] Phatiphat Thounthong, Stéphane Raël, and Bernard Davat "Control Algorithm of Fuel Cell and Batteries for Distributed Generation System", *IEEE Trans. on Energy Conversion,* vol.23, no 1, March 2008.

[7] Landau Ioan Doré, Langer Jochen, Ray Daniel, and Barnier. Jean. "Robust control of a 360o flexible arm using the combined pole placement/ sensitivity function shaping method", *IEEE Transaction on Control systems Technology*, Volume 4, Issue 4, pp.369-383, 1996.

[8] M.B.Camara, D.Fodorien, H.Gualous,D.Bouquain and A.Miroui, "Hybrid Sources Control for Electric Drives Traction Applications",*19th IEEE Int. Symposium on Power Electronics, Electrical Drives, Automation and Motion*, 11-13 June 2008, Ischia-Italy, Proceedings CD.

[9] Camara, M.B. Gualous, H. Gustin, F. and Berthon, A. "Experimental study of buck-boost converters with polynomial control strategy for hybrid vehicles applications", *International Review of Electrical Engineering* (*IREE),* vol.2, no 4, pp.601-612, August 2007

VII. Biographies

Dr. M. B. Camara was born in Guinea. He received the B.S. degree in engineering from the Polytechnic Institute of Conakry (IPC), Conakry, Guinea, in 2003 and the M.S. and Ph.D. degrees from the University of Franche-Comté, Belfort, France, in 2004 and 2007, respectively. Since 2004, he has been working in power electronics and electric vehicle research projects, involving static converter topologies, supercapacitors, batteries, and electrical energy management for hybrid vehicle applications. Since 2008, he is Associate Professor with the "Groupe de Recherche en Electrotechnique et Automatique du Havre: GREAH" Laboratory, University of Le Havre, France.

Pr. Brayima Dakyo (M'06) received the Dipl. Engineer degree and the Ph.D. degree in engineering from Dakar University, Dakar, Senegal, in 1984 and 1987, respectively, and the Ph.D. degree and Habilitation from The University of Le Havre, Le Havre, France, in 1988 and 1997, respectively. He is a Full Professor of electrical engineering and the Head of a research team at the "Groupe de Recherche en Electrotechnique et Automatique du Havre" Laboratory, University of Le Havre. His current interests include power electronics, converter-fed electrical machines, electrically powered systems, wind and solar energy systems, and diagnostics.

Pr. Cristian Nichita is an Electrical Engineer from Polytechnic Institute of Iasi - Romania (1977) and Doctor in Electrical Engineering from The University "Dunarea de Jos" of Galati – Romania (1996). He received his PhD degree (1995) and Research habilitation (2007) from University of Le Havre, France. He joined the Group of Research in Electrical engineering and Automatics, Le Havre (GREAH) in 2000. He is presently full Professor of Electrical Engineering at The University of Le Havre. His research interests include wind power systems, energy conversion and power in the loop simulation.